Appl. Phys. B 67, 347–350 (1998)

Applied Physics B
Lasers
and Optics

Compact mid-infrared trace gas sensor based on difference-frequency generation of two diode lasers in periodically poled $LiNbO_3$

D. Richter[1], D.G. Lancaster[1], R.F. Curl[1], W. Neu[2], F.K. Tittel[1]

[1] Rice Quantum Institute, Rice University, 6100 Main St., Houston, TX 77005, USA
(Fax: +1-713/524-5237, E-mail: fkt@rice.edu)
[2] Fachhochschule Ostfriesland - University of Applied Sciences, Constantiaplatz 4, D-26723 Emden, Germany

Received: 16 June 1998

Abstract. The development and characterization of a compact mid-infrared source for high-resolution spectroscopic detection of trace gases such as methane and water vapor at 3.3 μm in ambient air is reported. This source utilizes difference frequency generation (DFG) in a periodically poled $LiNbO_3$ (PPLN) crystal pumped by two single-frequency diode lasers. A maximum DFG power of 1.6 μW at 3.6 μm was generated with a pump power of 61.4 mW at 832 nm and a signal power of 41.5 mW at 1083 nm incident on a 19-mm-long PPLN crystal, which corresponds to a conversion efficiency of 335 $\mu W\,W^{-2}\,cm^{-1}$.

PACS: 7.65; 42.60B; 42.80

The motivation for this work has been the need to develop a robust, compact and consumable-free sensor for the sensitive and selective detection of pollutants and environmentally important trace gas species in ambient air. To accomplish this, numerous optical and non-optical techniques have been developed. However, the advent of novel enabling technologies involving room-temperature diode lasers, efficient nonlinear optical materials, optical fibers and non-cryogenic infrared detectors has made it possible to investigate a new device architecture for laser-based DFG gas sensors that is particularly suited for the 3–5 μm spectral region. This approach allows access to considerably stronger fundamental ro-vibrational absorption lines rather than weaker overtone molecular transitions for convenient gas monitoring by means of direct absorption spectroscopy. The design issues of an infrared spectrometer based on DFG were considered previously in [1, 2]. Several groups have demonstrated DFG by mixing two laser diodes in $AgGaS_2$ [3–5], which resulted in IR power levels of tens of nanowatts. The recent commercial availability of periodically poled $LiNbO_3$ (PPLN) allows the use of a high nonlinear coefficient $d_{33} = 24\,pm/V$ [6, 7] and convenient DFG quasi-phase-matching (QPM) of diode-laser pump sources.

1 Experimental details and sensor optimization

In a second-order nonlinear DFG process the two incident waves, customarily called pump (ω_p) and signal (ω_s), are frequency down-converted to generate the idler beam (ω_i) in accordance to the relation $\omega_i = \omega_p - \omega_s$. The schematic layout of the DFG-based sensor is shown in Fig. 1. A distributed Bragg reflector (DBR) type diode laser ($P = 50$ mW) and Fabry–Pérot (FP) GaAlAs diode laser ($P = 100$ mW) are collimated and spatially overlapped via a dichroic beamsplitter. The center wavelength of the DBR diode laser (signal) is at 1083 nm whereas FP diode lasers (pump) are available with center wavelengths ranging from 810 nm to 865 nm and a typical gross tuning range of ±3 nm [8, 9]. This leads to an overall DFG spectral coverage from 3.2 μm to 4.3 μm, which corresponds to a region of optimum optical transmission of PPLN [10]. After passing through an anamorphic prism pair (3×), the beams are focused by a plano-convex lens of 38 mm focal length into a 19-mm-long PPLN crystal. The DFG beam

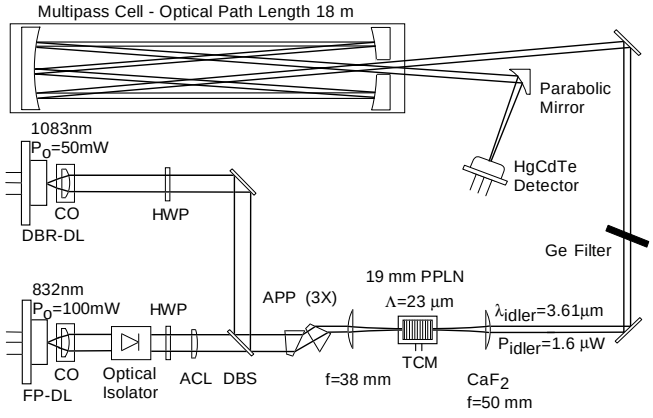

Fig. 1. Schematic of the diode-laser-based mid-infrared DFG sensor. CO, collimation optic; HWP, half wave plate; ACL, astigmatism correction lens; DBS, dichroic beam splitter; APP, anamorphic prism pair; TCM, temperature-controlled PPLN crystal mount

is collimated by a CaF_2 lens (50 mm focal length). A germanium filter with a cut-off wavelength of 2 μm removes the non-converted input pump beams. The DFG beam is then directed into a multi-pass spectroscopic cell configured to a 18-m effective optical path length. The output beam from the cell is focused onto a thermo-electrically cooled HgCdTe (MCT) detector by an off-axis parabolic mirror. The signal of the calibrated MCT detector is amplified by a low-noise DC-coupled preamplifier with a measured noise equivalent power of 8 pW/$\sqrt{\text{Hz}}$, providing a signal-to-noise ratio of five orders of magnitude.

Two FP diode lasers with different center wavelengths were investigated in combination with two different PPLN crystals: first, a PPLN crystal of 19 mm length with a QPM grating period of $\Lambda = 23.0\,\mu\text{m}$ and a 832-nm FP diode laser, and second a multi-channel grating PPLN crystal ($\Lambda =$ 22.5–23.1 μm) of 20 mm length and a 817-nm FP diode laser were used. Both end surfaces of the crystal were anti-reflection coated at the pump and DFG wavelengths. QPM for a defined wavelength range can be conveniently maintained by using active temperature control or a multi-channel grating PPLN crystal or combinations of both. Alternatively, a grating design with a fan-out grating pattern [11] can be used. The incremental grating period channel difference of a multi-channel crystal is 0.1 μm. If no active temperature control is used the crystal can be slightly tilted for fine QPM adjustments. However, tilting of the PPLN crystal introduces a beam walk-off, resulting in loss of spatial beam overlap and a decrease of DFG power. In this sensor, the difference between the nominal (grating period of the crystal at room temperature) and the required grating period was adjusted by using a temperature-controlled mount that consisted of an integrated single-stage Peltier element with a 10-KΩ (at 25 °C) thermistor for temperature readout. Figure 2 shows the computed tuning characteristic of the quasi-phase-matched PPLN mixing crystal at different temperatures. The degeneracy point at which one obtains the largest phase-matching bandwidth is located at a pump wavelength of 858 nm for a fixed signal wavelength of 1083 nm. At 24.5 °C, the calculated PPLN degeneracy

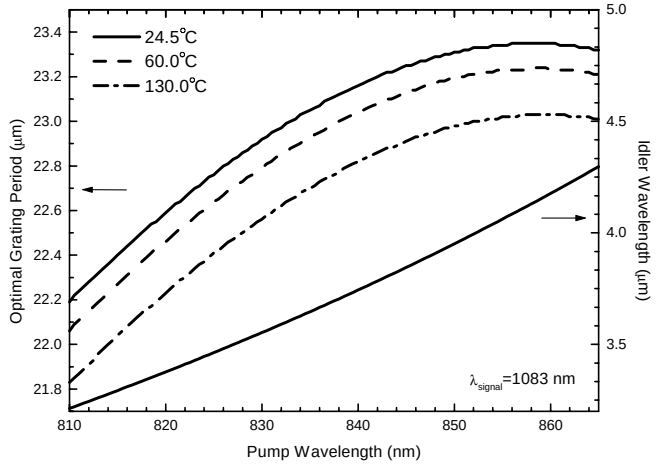

Fig. 2. Computed tuning characteristic of a quasi-phase-matched PPLN crystal at a fixed signal wavelength of 1083 nm. Shown is the optimal grating period at three temperatures of 24.5, 60, and 130 °C and the generated idler wavelength as a function of the pump wavelength

phase-matching bandwidth at FWHM is 121 cm^{-1}, which allows broad DFG tuning centered at ∼ 4 μm without the need to adjust the phase-matching conditions. For pump wavelengths longer or shorter than ∼ 858 nm, the adjustment of the phase-matching condition can be achieved conveniently by using temperature tuning. For example, a pump wavelength of 833 nm and signal wavelength of 1083 nm can be phase-matched with a computed optimal grating period of 23.0 μm at $T = 24.5\,^{\circ}\text{C}$, equal to the nominal grating period of the available PPLN crystal. By implementing a resistive heater element, the temperature of the PPLN crystal could be increased further so that pump wavelengths from 833 nm at $T = 24.5\,^{\circ}\text{C}$ to 865 nm at $T = 130\,^{\circ}\text{C}$ could be phase-matched with a $\Lambda = 23.0\,\mu\text{m}$ grating period at a signal wavelength of 1083 nm.

Minimization of the beam propagation factor M^2 [12] was found to be significant in achieving optimum nonlinear optical conversion in the PPLN crystal. Various diode-laser collimating optics were compared in order to evaluate their suitability by measuring the M^2 factor in both the horizontal and the vertical planes. Multi-element as well as various aspheric lenses were tested. Beam waists for both diode lasers in the horizontal and vertical plane were measured by using a plano-convex lens with a 70-mm focal length. The beam size was measured along the optical axis with a CCD camera mounted on a translation stage and the beam propagation factor calculated from the measurement of beam size as a function of distance. Table 1 shows the M^2 values of tested collimation optics. The lenses are corrected for aberration effects due to the window of the hermetically sealed laser diode package (TO-3). Furthermore, the high numerical aperture of the aspheric collimation lenses truncates less of the power in the wings of the beam, resulting in reduced beam diffraction effects. In addition an astigmatic correction lens was introduced into the optical path of the FP diode laser to compensate for astigmatism. Then the DFG efficiency of the three sets of optics was measured and the use of single aspheric lenses (Geltech) with a focal length of 4.5 mm and a numerical aperture of 0.55NA was found to yield the best DFG efficiency along with a best compromised M^2 value.

The optimized diode-laser-pumped DFG sensor reported here generated as much as 1.6 μW with input powers of 41.5 mW and 61.4 mW at 1083 nm and 832 nm, respectively, at the PPLN crystal input facet. This corresponds to a conversion efficiency of 335 $\mu\text{W}\,\text{W}^{-2}\,\text{cm}^{-1}$. The theoretically calculated DFG power is 3.42 μW and can be derived from the expression in [13] applicable to focussed Gaussian beams.

This implies that the sensor can operate with a conversion efficiency of 47% with respect to the theoretically computed

Table 1. M^2 of collimation optics for DFG pump laser diodes in the horizontal (//) and the vertical (⊥) planes

	DBR		FP	
	//	⊥	//	⊥
Multi-element 0.5NA, $f = 8$ mm	6.56	3.86	5.03	6.80
Aspheric 0.65NA, $f = 2.75$ mm	1.65	4.60	1.89	13.6
Aspheric 0.55Na, $f = 4.5$ mm	1.58	5.90	1.72	5.98

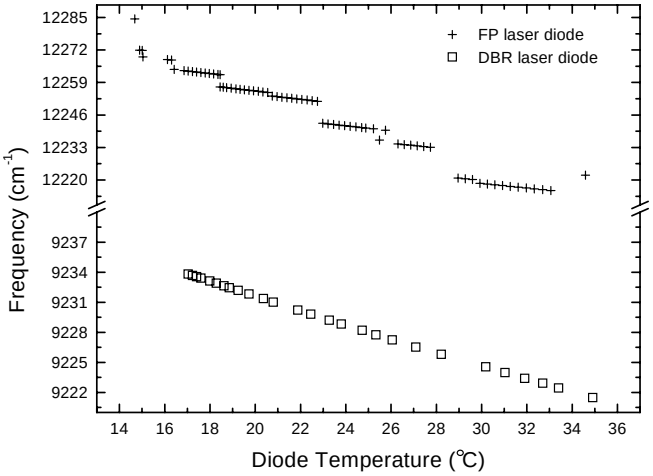

Fig. 3. Diode laser wavelength tuning characteristics: frequency vs. diode laser temperature

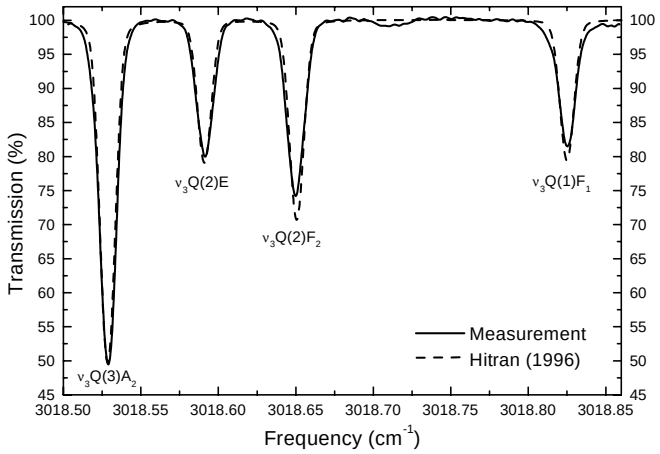

Fig. 4. CH_4 spectrum in the Q branch at 3.31 μm. A small volume of methane was added to the gas-handling unit. The multi-pass cell was then sealed for spectral measurements at a pressure of 10 Torr

value. The DFG power was corrected for reflection losses at the surfaces of the CaF_2 beam collection lens (5.9%) and the germanium filter (6.7%).

A spectroscopically important characteristic of this sensor is its capability to fine tune both pump diode lasers to access the mid-IR absorption lines of selected target gas species. The frequency outputs of both diode lasers were measured with a wavemeter (Burleigh WA-1000, 0.01 cm^{-1} absolute accuracy) for a diode temperature range of ∼ 17 °C as shown in Fig. 3. The DBR diode laser was continuously tunable over ∼ 6 cm^{-1}, while the FP diode laser had a gross tuning range of ±25 cm^{-1} around its center wavelength at 817 nm. The gross tuning range of Fabry–Pérot-type diode laser is typically interrupted by mode hops. This limits the accessibility of absorption lines to mode-hop-free regions if one of the other pump sources cannot be tuned. In this sensor design, the DBR diode laser can be used to compensate the FP diode laser frequency by an appropriate current–temperature adjustment strategy to a line without mode hopping [14].

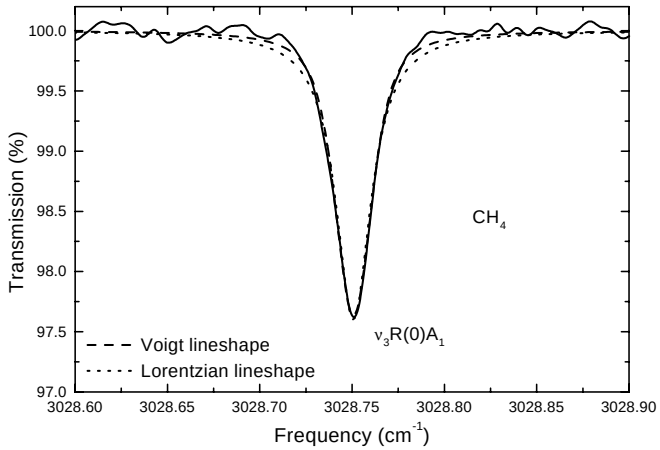

Fig. 5. Interference-free absorption line of CH_4 at 3028.751 cm^{-1} obtained with a calibrated gas sample [NOAA, 1998] at a pressure of 100 Torr

2 Spectroscopy results

The high-resolution spectroscopy capability of this sensor was evaluated for methane and water vapor near 3.3 μm. A compact gas-handling unit consisting of an in-line pressure regulator and a miniature diaphragm pump was connected to the multi-pass cell. Spectral data at reduced pressures ranging from 100 Torr down to 10 Torr were acquired. Operating at reduced pressure improves the selectivity by reducing the pressure broadening without affecting concentration measurements and decreasing interference from other gases present. Shown in Fig. 4 is a portion of the Q-branch spectrum at 3018 cm^{-1} (3.31 μm) of the ν_3 band of methane (10 Torr) and the computed spectrum from the Hitran molecular spectroscopic database [15]. The linewidth for the CH_4 transition at 3018.529 cm^{-1} was measured to be 307 MHz. The linewidth of the DFG probe beam is estimated to be less than 150 MHz from deconvolving the computed and recorded spectra by assuming a Gaussian lineshape. For methane the Doppler-limited linewidth is 280 MHz at 3.31 μm. An absorption line at 3028.751 cm^{-1} was chosen for methane concentration measurements (Fig. 5). This line is relatively free of interference by other gas species except for a weak water absorption peak at 3028.877 cm^{-1}, which has an absorption 10 times lower than that for a 1.78-ppm CH_4 absorption (48% relative humidity, 24.5 °C) and would not affect the measured CH_4 concentration. A calibrated gas mixture [16] containing CH_4, CO_2, CO, and N_2O was passed through the multipass cell at 100 Torr pressure. Using a line strength of $S = 9.519 \times 10^{-20}$ cm/molecule [15], the sensor measured a CH_4 concentration of 1.790 ppm as depicted in Fig. 5 for the calibrated value of 1.773 ppm. The water line at 3028.877 cm^{-1} does not appear since a dry-calibrated gas mixture was used. To remove the baseline of the spectral scan a fifth-order polynominal fit was used and a Lorentzian lineshape was fitted to the absorption peak using a Levenberg–Marquardt least-squares fit procedure [17]. However, the real-time Lorentzian fitting procedure at a probing pressure of 100 Torr leads to a slight fitting discrepancy in the wings of the CH_4 absorption line and the line is therefore more appropriately fitted by a Voigt lineshape, as can be seen from Fig. 5. At present, our sensor does not provide real-time Voigt profile fitting but efforts are under way to implement a real-

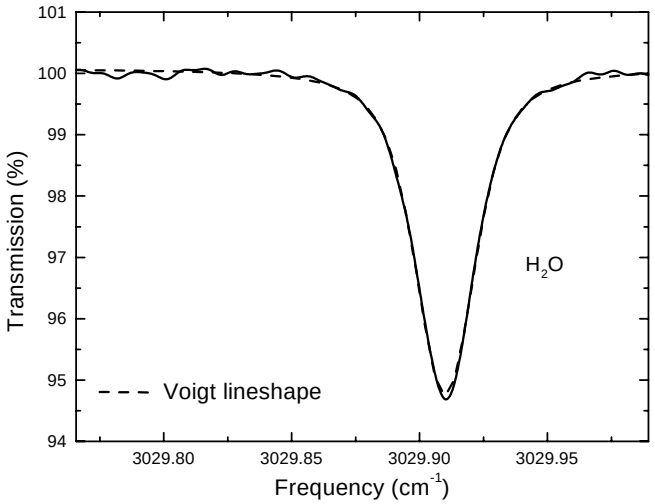

Fig. 6. H_2O absorption line at 3029.91 cm^{-1} measured in ambient air at 100 Torr

time Voigt fitting procedure. A water vapor absorption line was measured at 3029.91 cm^{-1} as shown in Fig. 6 from which a relative humidity of 48% at 24.5 °C was computed using a linestrength of $S = 2.930 \times 10^{-23}$ cm/molecule [15].

In summary, a compact, narrow linewidth, tunable spectroscopic source based on difference frequency generation in PPLN pumped by two single-frequency diode lasers for the detection of high-resolution spectra of methane and water vapor has been demonstrated. Once aligned, the sensor operates for a long period of time (days) in a laboratory environment without requiring realignment. No warm-up time was needed to reactivate the sensor if it was switched off. This sensor can be made more robust for field use by replacing discrete optics by fiber coupling, and more sensitive by adding in-line fiber amplifiers to boost DFG power [18], which will permit the use of signal-to-noise enhancement techniques like balanced detection schemes.

Acknowledgements. DR would like to acknowledge a stipend from the German Academic Exchange Service (DAAD) to complete his diploma thesis at Rice University. Financial support was provided by NASA, the Texas Advanced Technologies Program, the National Science Foundation, and the Welch Foundation.

References

1. U. Simon, Z. Benko, M.W. Sigrist, R.F. Curl, F.K. Tittel: Appl. Opt. **32**, 33 (1993)
2. Th. Töpfer, K.P. Petrov, Y. Mine, D. Jundt, R.F. Curl, F.K. Tittel: Appl. Opt. **36**, 8042 (1997)
3. U. Simon, C.E. Miller, C.C. Bradley, R.G. Hulet, R.F. Curl, F.K. Tittel: Opt. Lett. **18**, 13 (1993)
4. B. Sumpf, T. Kelz, M. Nägele, H.-D. Kronfeldt: Appl. Phys. B **64**, 5 (1997)
5. W. Schade, T. Blanke, U. Willer, C. Rempel: Appl. Phys. B **63**, 1 (1996)
6. L. Goldberg, W.K. Burns, R.W. McElhanon: Opt. Lett. **20**, 11 (1995)
7. D.H. Jundt: Opt. Lett. **22**, 20 (1997)
8. Spectra Diode Labs (SDL), Technical Notes (1997)
9. C. Wieman, L. Hollberg: Rev. Sci. Instrum. **62**, 1 (1991)
10. L.E. Myers, R.C. Eckardt, M.M. Fejer, R.L. Byer, W.R. Bosenberg: Opt. Lett. **21**, 8 (1996)
11. P.E. Powers, Th.J. Kulp, S.E. Bisson: Opt. Lett. **23**, 3 (1998)
12. A.E. Siegman: OSA TOPS Vol. 17, p. 184 (1998)
13. P. Canarelli, Z. Benko, R. Curl, F.K. Tittel: J. Opt. Soc. Am. B **9**, 2 (1992)
14. R.S. Putnam, D.G. Lancaster: "A cw laser spectrometer automatically aligned and continuously tuned from 11.8–16.1 μm using diode laser pumped difference frequency generation in GaSe", accepted by Appl. Opt. (1998)
15. HITRAN 96, Ontar Corporation, North Andover, MA
16. Courtesy of E. Dlugokencky, NOAA, Climate Monitoring & Diagnostic Laboratory, Boulder, CO
17. D.G. Lancaster, D. Richter, R.F. Curl, F.K. Tittel: Appl. Phys. B **67**, 339 (1998)
18. D.G. Lancaster, L. Goldberg, J. Koplow, R.F. Curl, F.K. Tittel: Electron. Lett. 1345 (1998)